

## Can flow bursts penetrate into the inner magnetosphere?

S. Dubyagin,<sup>1</sup> V. Sergeev,<sup>1</sup> S. Apatenkov,<sup>1</sup> V. Angelopoulos,<sup>2</sup> A. Runov,<sup>2</sup> R. Nakamura,<sup>3</sup> W. Baumjohann,<sup>3</sup> J. McFadden,<sup>4</sup> and D. Larson<sup>4</sup>

Received 6 February 2011; revised 4 March 2011; accepted 8 March 2011; published 19 April 2011.

[1] Recent studies have shown that only a small fraction of fast-flow bursts observed at mid-tail penetrate into the inner magnetosphere, raising questions regarding their role in particle injections. Motivated by these findings, we compared observations at two radially-aligned Time History of Events and Macroscale Interactions during Substorms (THEMIS) spacecraft in the high-beta nightside plasma sheet to determine which physical parameter controls the penetration efficiency of flow bursts observed at the outer spacecraft. We showed that the inferred plasma tube entropy  $PV^{5/3}$  demonstrates better prediction efficiency than other parameters (e.g.,  $V_x$  or  $B_z$ ). Comparing its minimal value at the outer spacecraft during the flow burst to its preflow value at the inner spacecraft allows us to distinguish between penetrating and non-penetrating events. Our results explain the relatively small number of deeply penetrating BBFs and provide a strong argument in favor of the bubble model of fast-flow bursts and plasma injections. **Citation:** Dubyagin, S., V. Sergeev, S. Apatenkov, V. Angelopoulos, A. Runov, R. Nakamura, W. Baumjohann, J. McFadden, and D. Larson (2011), Can flow bursts penetrate into the inner magnetosphere?, *Geophys. Res. Lett.*, **38**, L08102, doi:10.1029/2011GL047016.

### 1. Introduction

[2] Narrow Earthward plasma jets or bursty bulk flows (BBFs) are known to be the major contributor to plasma transport in the magnetotail plasma sheet [Angelopoulos *et al.*, 1992]. They are also believed to be responsible for near-Earth dipolarization and energetic particle injection into the inner magnetosphere. Recent studies using concurrent observations at two radially-separated spacecraft found an unambiguous connection with near-Earth dipolarizations in only a small fraction of BBFs in the mid-magnetotail [Ohtani *et al.*, 2006; Takada *et al.*, 2006]. According to these authors, generation of fast flow in the magnetotail (regardless of its velocity or magnetic flux transport rate) is insufficient to cause near-Earth dipolarization. Another BBF parameter may control penetration into the inner region, however.

[3] Pontius and Wolf [1990] suggested a “plasma bubble” model to explain BBFs in the magnetotail (see Wolf *et al.*

[2009] for a recent review). The authors show that if a flux tube has an entropy ( $S = PV^{5/3}$ , where  $V$  is the volume of the unit magnetic flux tube) smaller than that of surrounding plasma, this “plasma bubble” is subject to interchange instability and will move Earthward. Most observed BBFs have an increased magnetic field and reduced plasma pressure [e.g., Ohtani *et al.*, 2004]. From the plasma bubble viewpoint the question about penetration depth has, at first glance, a simple answer (see the scheme in Figure 1a). The plasma tube entropy  $S$  increases monotonically with distance in the background magnetotail plasma [Wolf *et al.*, 2009]. The bubble is expected to move Earthward adiabatically, conserving its reduced entropy ( $S_b$ ), until the background plasma entropy equals  $S_b$ . At this point the bubble stops. While perhaps idealized, this model can nonetheless be tested. This is the main purpose of our paper.

[4] We take advantage of possibilities fortuitously provided by the THEMIS mission [see Sibeck and Angelopoulos, 2008, and references therein]. Among other elements, THEMIS employs a group of 3 identical near-Earth magnetosphere spacecraft in equatorial orbits (apogees 10–12  $R_E$ ). In the 2008 magnetotail season these spacecraft (probes P3, P4, P5) frequently formed nearly radial configurations with separations of  $\sim 2 R_E$  (see Figure 1b). This small separation increases the chance of BBF passage through both probe locations while still having background entropy values considerably different at each of them (Figure 1c). The distance range for most crossings (8–11  $R_E$ ) corresponds to the region where, according to previous studies, most BBFs are stopped [Takada *et al.*, 2006; Ohtani *et al.*, 2006].

### 2. Event Selection and Examples

[5] We used spin-averaged observations made by the THEMIS probes, including magnetic and electric field data (from FGM and EFI instruments, respectively) and particle observations by ESA and SST instruments, which together cover the 5 eV to >900 keV energy range. The plasma pressure was computed by summing contributions from ESA and SST; the ion velocity was computed from ESA data only. We required that two THEMIS probes be in the local time sector 21–03 h MLT at distances between 5 and 12  $R_E$ . To select events with probe alignment nearly along the radial direction, we require that the azimuthal separation be within 0.25 hour MLT (or  $\Delta Y < 0.5 R_E$  at  $\sim 8 R_E$  distance) and that radial separation be  $> 1 R_E$  (on average,  $\sim 2 R_E$ ). To keep both probes near the equatorial plane (for more accurate entropy estimation), we additionally require  $|B_{xNS}/B_{zNS}| < 1.5$ , where the magnetic field components are in a neutral sheet coordinate system (NS), with Z along a model NS normal [Tsyanenko and Fairfield, 2004] and the X, Y, Z components near the nominal GSM directions but adjusted to account for NS tilt and warping (see Dubyagin *et al.*

<sup>1</sup>Earth Physics Department, St. Petersburg State University, St. Petersburg, Russia.

<sup>2</sup>Institute of Geophysics and Planetary Physics, University of California, Los Angeles, California, USA.

<sup>3</sup>Space Research Institute, Austrian Academy of Sciences, Graz, Austria.

<sup>4</sup>Space Sciences Laboratory, University of California, Berkeley, California, USA.

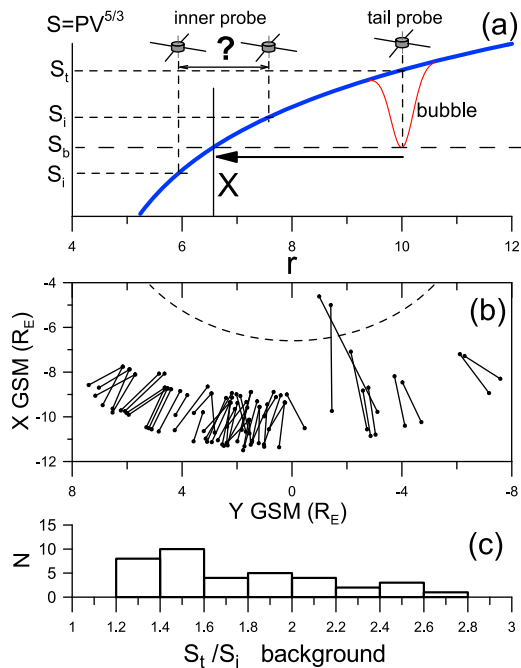


**Figure 1.** (a) Illustrative sketch: radial profile of entropy parameter  $S = PV^{5/3}$  of background plasma sheet (blue thick curve) and plasma bubble (thin red curve). See explanations in the text. (b) Spatial distribution of events in XY GSM plane. Dashed curve shows geostationary orbit. (c) Histogram of the ratio of background entropy at tail probes to entropy at inner probe.

[2010] for more details). This was particularly important when calculating the plasma tube entropy  $S$  using equations (6,9,11) of *Wolf et al.* [2006], which use as input the  $B_z$  and  $B_r$  magnetic field components in the current sheet coordinate system as well as the measured plasma pressure value. The event selection procedure is an important part of this study. According to previous studies [e.g., *Schödel et al.*, 2001], flow burst velocity decreases significantly towards the inner magnetosphere, where the flux transport rate can still be significant, due to enhanced  $B_z$ . The electric field  $|E_{xy}|$  is a better parameter to identify flow bursts in the near-Earth tail region at  $\sim 10R_E$ . Therefore we identified time intervals at the outer probes that display considerable flux transport,  $\delta|E_{x,y}| \geq 1$  mV/m, where  $\delta E$  refers to electric field variation during a 30 sec interval. This condition does not require offset subtraction from EFI data. The intervals of enhanced flux transport with isolated onset (non-disturbed background for more than 3 minutes) were then inspected to confirm  $B_{zNS}$ -component increase above 4 nT over the 30 sec time interval (dipolarization). No condition was imposed on the flow velocity during selection. In the resulting dataset about 40% of events had  $V_{\perp xy} > 300$  km/s ( $> 100$  km/s in 91%), and in 67% of events  $[B \times V]_y > 2$  mV/m.

[6] A basic signature with which to identify flow burst arrival at the inner region is energetic particle flux increase (by more than a factor of 2 in 1 minute in more than two energy channels) at the inner probe. A small drift dispersion is allowed, so that we are also able to capture injections that occurred aside of the probe. This is essential because the actual trajectory of the flow burst (which is narrow, about  $2-3R_E$  [*Nakamura et al.*, 2004]) is difficult to control.

By relying on dipolarization signatures only, the inner spacecraft could miss flow injection. Ninety percent of the events in our database had a radial separation  $\Delta r < 3R_E$ ; it takes only  $\sim 3$  minutes for a typical flow burst to cover this distance at 100 km/s. The absence of a sharp increase in energetic ion or electron fluxes during the interval  $[t_0 - 1 \text{ min}, t_0 + 3 \text{ min}]$  was therefore considered as a signature that the BBF stopped somewhere between the two probes. Two events shown in Figure 2 illustrate the selection procedure and differences between the two types of behavior. In each case the inner probe was at  $r \approx 9R_E$ , and the tail probe was at  $r \approx 11R_E$ . At the tail probe the BBF, which was initially recognized from EFI measurements, was accompanied by flow bursts and magnetic field dipolarization. In Figure 2, the beginning of magnetic field perturbation at the tail probe is indicated by a vertical solid line and referenced hereinafter as  $t_0$  time. Although observed tail probe variations are similar, observed inner probe variations are very different. After a  $\sim 50$  sec delay, the sharp dipolarization front at the tail probe was followed by a corresponding dipolarization front at the inner probe for the 23 February 2008 event. Dipolarization at the inner probe was accompanied by a sharp electron flux increase, a good example of a flow penetrating event. In this event the entropy  $S$  at the tail probe dropped below its value at the

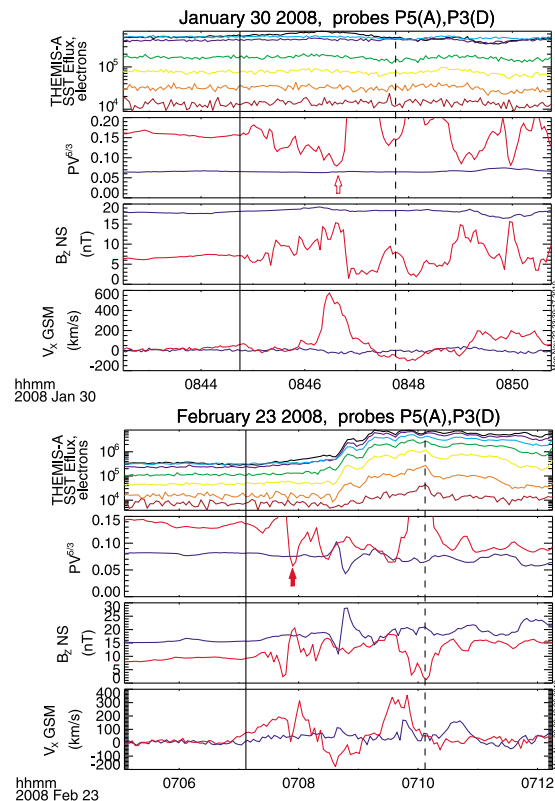


**Figure 2.** Two examples of THEMIS observations. (top) SST energy flux variations (in 30/41/53/67/95/142/207 keV channels) observed by inner-probe. (bottom) Combination of observation from inner-probe (blue curve) and tail-probe (red curve). From top to the bottom: entropy parameter (in  $\text{nPa}(R_E/\text{nT})^{5/3}$ );  $B_z$  in neutral sheet coordinates; X GSM component of plasma velocity. Vertical lines mark start time ( $t_0$ ) and  $t_0 + 3$  min. time.

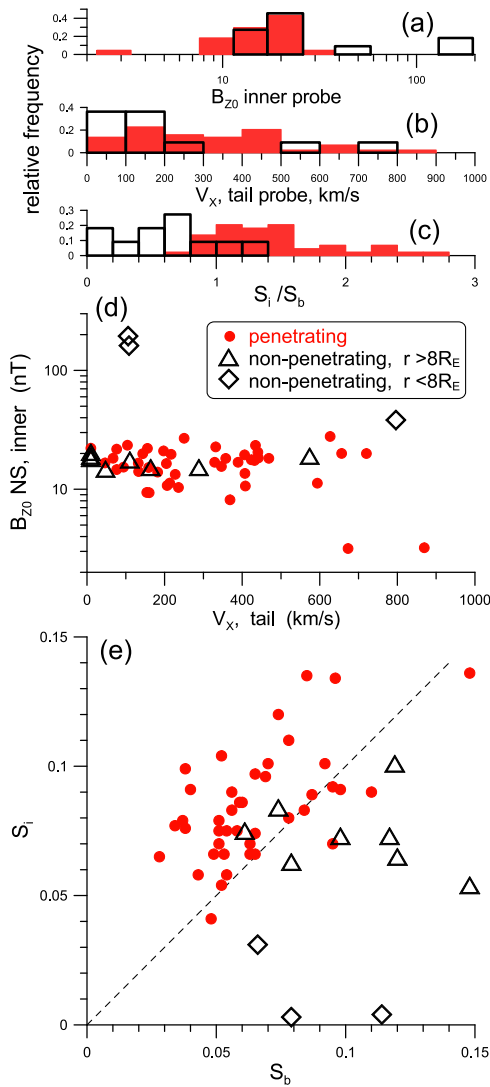


**Figure 3.** Frequency distribution for penetrating (red) and non-penetrating (black) events of: (a) background  $B_{zNS}$  at the inner probe at  $t = t_0$ ; (b) maximum value of X GSM component of ion bulk flow at the tail probe between  $t_0$  and  $t_0 + 3$  min; (c) ratio of entropy at inner probe ( $S_i$ ) at  $t = t_0$  to the minimum entropy at tail probe ( $S_b$ ) during  $[t_0, t_0 + 3]$  min interval. (d) Background  $B_{zNS}$  at inner probe versus maximum X GSM component of plasma velocity at tail probe. (e) Background entropy at inner probe versus bubble entropy.

inner probe (red arrow), so bubble penetration corresponds to the bubble model prediction. However, no dipolarization or injection signatures are seen in SST electron data for the 30 January 2008 event (ion SST data also show no variations). This case provides an example of a “non-penetrating event”; note that an observed entropy reduction at the tail probe (red arrow) is still above the value calculated at the inner probe. Interestingly, Earthward flow velocity on the tailward probe is higher ( $V_x \sim 600$  km/s) for the non-penetrating event than for the penetrating event ( $\sim 300$  km/s), demonstrating that flow speed is not a good predictor of the fate of the flow burst.

[7] Applying the criteria described in the previous section to observations during THEMIS tail seasons 2007–2009,

we selected 55 events whose spatial distribution is shown Figure 1b. In 72% of events the probes were separated by  $1.5 < \Delta r < 2.5R_E$ . Background entropies at the inner ( $S_i$ ) and tail probes ( $S_t$ ) were determined during a few undisturbed minutes prior to  $t_0$ . The ratio of background entropies at the tail and inner probes  $S_t/S_i$  in Figure 1c shows that the average entropy increases by more than 50% over  $\sim 2R_E$ , which is consistent with empirical models [Wolf *et al.*, 2009]. In addition, the minimal entropy value at the tail probe between  $t_0$  and  $t_0 + 3$  min is used as an estimate of the  $S_b$  - bubble entropy. The background entropy at the inner probe ( $S_i$ ) was determined at time  $t_0$ .

[8] Of the 55 events, only 11 non-penetrating ones without flow burst signatures at the inner probe were recorded. Hence, our flow burst “success rate” is about 80%, more than twice as large as the approximately 30% at  $\sim 5R_E$  separation in Takada *et al.*’s [2006] study. Following the findings of these authors that penetration efficiency is lower when the magnetic field is strong at the inner probe, we show in Figure 3a histograms for background  $B_{zNS}$  at the inner probe for penetrating and non-penetrating events. In all 3 cases of strong  $B_z$  ( $>40$  nT), the BBF was unable to penetrate. However, this parameter has a weak prediction efficiency: the number of penetrating and non-penetrating events is largest in the same 10 nT to 40 nT bins and is similar for both types of events. Figure 3b shows histograms of the maximum  $V_x$  observed at the tail probe from  $t_0$  to  $t_0 + 3$  min. One might have expected this parameter to be a significant controller of inward plasma penetration, but this is not true, as there is no clear separation between the two velocity distributions. To avoid interplay between these two parameters, we plotted the event distribution in  $V_x$  vs  $B_{zNS}$  coordinates (Figure 3d), which supports the above conclusions. Histograms of the  $S_i/S_b$  ratio for the two groups of events (Figure 3c) show that non-penetrating events occupy the  $S_i/S_b < 1$  region, and penetrating events occupy the  $S_i/S_b > 1$  region preferentially. Only 2 non-penetrating events ( $\sim 15\%$ ) get into the  $S_i/S_b > 1$  part, and only 7 penetrating events (15%) get into the  $S_i/S_b < 1$  part. The conclusion is further supported by plotting distributions in  $S_i$  versus  $S_b$  coordinates in Figure 3e. It should be noted that Wolf *et al.*’s [2006] formula is an approximation of a number of equilibrium models, and its accuracy is difficult to control in every specific case. Nevertheless, the flux tube entropy values estimated in that way show clear physical dependence.

### 3. Discussion

[9] The flow-braking process is neither well-studied observationally, nor well-understood. Previous discussions have suggested that the BBF plasma jet may stop suddenly at the junction of the neutral sheet tail current and the magnetic wall (increasing  $B_z$ ) region, at around  $10 R_E$  [Shiokawa *et al.*, 1997]. The low penetration efficiency of BBFs to the inner tail region together with the lack of penetration efficiency sensitivity to the flow burst magnitude [Ohtani *et al.*, 2006; Takada *et al.*, 2006] seem to support the view that most flow bursts are stopped somewhere in that region. Our results complement this view, showing that even with a  $2 R_E$  separation between the probes, a significant fraction (23%) of all flow bursts do not penetrate Earthward of  $\sim 9R_E$ , the typical location of

the inner probe in our database. Our results provide additional information regarding the plasma injection process: only fast streams with suitably small entropy can reach the inner region. In agreement with conclusions from bubble MHD simulations [Birn *et al.*, 2009, Figure 10] we conclude that the loss of entropy is the most significant factor enabling closed flux tubes to penetrate into the inner magnetosphere. Neither initial flow velocity, nor magnetic field strength can compete with the entropy parameter in predicting penetration depth.

[10] The wide distribution of entropy depletion values and of corresponding penetration distances might explain the statistical decrease in mass and entropy content of magnetic flux tubes from the tail toward the Earth noticed in previous studies [Wolf *et al.*, 2009]. Two more recent studies further support this view. A THEMIS-based study of dipolarizations in the near-Earth region (down to  $6 R_E$ ) demonstrated statistically that the entropy and plasma tube content are systematically reduced in post-dipolarization plasma [Dubyagin *et al.*, 2010]. A superposed epoch analysis of Geotail observations at the entry to the dipole-like region by Yang *et al.* [2010] showed that during substorms and steady convection, plasma tube entropy is reduced to a value characteristic of the near-geostationary orbit environment, suggesting that plasma could be injected into the geosynchronous orbit distance under such conditions, which is consistent with our observations. However, there are also clear deviations from the simplest version of the bubble hypothesis. The ideal filamentary bubble barely disturbs the surrounding media as it moves through. In reality, plasma flow, density, and pressure increase smoothly for  $\sim 1$  min prior to arrival of the bubble's sharp leading front [Ohtani *et al.*, 2004; Dubyagin *et al.*, 2010; Li *et al.*, 2011]. This compression of background plasma (as distinct from bubble plasma, which has a different entropy [Dubyagin *et al.*, 2010]) and associated pressure pileup in the inner region have been demonstrated to be associated with BBF deflection and rebound [Panov *et al.*, 2010]. This rebound motion perhaps may partly explain why there is no one to one correspondence between amount of entropy reduction and flow speed as can be noticed in Figure 2. In line with simulation results [Birn *et al.*, 2009], we believe that these two effects, a "penetration through" mode of (narrow) bubble inward motion and pileup of background plasma pressure by (wide) plasma jet, should actually work together; their relative importance may depend on the effective width of the plasma bubble. These results support the view [Birn *et al.*, 2009; Wolf *et al.*, 2009] that plasma injection into the inner magnetosphere can be understood as a result of two basic interacting processes, magnetic reconnection and plasma tube interchange motions. Reconnection cuts plasma tube volume and introduces low-density lobe plasma into the plasma sheet, reducing plasma tube entropy and creating bubbles. The resultant interchange motion brings the bubble Earthward, up to a distance determined by entropy reduction in the bubble. Favorable conditions for deep penetration are (1) reconnection of lobe field lines (decreasing plasma density and pressure) and (2) Reconnection proximity to Earth (resulting in drastic reduction in volume). These conditions combined are able to drastically reduce the plasma tube entropy, and are typically realized during substorms, i.e., precisely when intense injections into the inner magnetosphere take place. Another condition to get BBFs closer to

Earth is to inflate the magnetic configuration (that is, to move the background profile  $S(r)$  in Figure 1a) closer to the Earth; this is consistent with Takada *et al.*'s [2006] findings.

[11] One may doubt the value of bubble formalism in the inner region where, because of increasingly important magnetic drifts, the "frozen-in" plasma tube approximation is no longer valid and bubble plasma is mixed with surrounding plasma, dissolving the bubble [Wolf *et al.*, 2009]. Three factors/processes are noteworthy in this context. First, a finite time to dissolve the bubble is controlled by magnetic drift, which takes some minutes to complete. Second, currents in and around the bubble may modify, cancel, or reverse the radial  $B$ -gradient (for example, it is reversed at the front of  $B_z$  increase). Third, bubble structure [Birn *et al.*, 2009] and instabilities of its frontside boundary [TanDokoro and Fujimoto, 2005] may help mix it with surrounding plasma. The result of these competing processes is not immediately apparent; simulations are required to adequately investigate these effects.

[12] **Acknowledgments.** We acknowledge K. H. Glassmeier, U. Auster, for the use of FGM data provided under the lead of the Technical University of Braunschweig and with financial support through the German Ministry for Economy and Technology and the German Center for Aviation and Space (DLR) under contract 50 OC 0302. We thank Judy Hohl for her editorial assistance in manuscript preparation. SD, VS and SA work was supported by SPSU grant and RFBR grant 10-05-00223. US support under THEMIS contract NAS5-02099 is also acknowledged.

[13] The Editor thanks two anonymous reviewers for their assistance in evaluating this paper.

## References

- Angelopoulos, V., W. Baumjohann, C. F. Kennel, F. V. Coroniti, M. G. Kivelson, R. Pellat, R. J. Walker, H. Lühr, and G. Paschmann (1992), Bursty bulk flows in the inner central plasma sheet, *J. Geophys. Res.*, *97*(A4), 4027–4039.
- Birn, J., M. Hesse, K. Schindler, and S. Zaharia (2009), Role of entropy in magnetotail dynamics, *J. Geophys. Res.*, *114*, A00D03, doi:10.1029/2008JA014015.
- Dubyagin, S., V. Sergeev, S. Apatenkov, V. Angelopoulos, R. Nakamura, J. McFadden, D. Larson, and J. Bonnell (2010), Pressure and entropy changes in the flow-braking region during magnetic field dipolarization, *J. Geophys. Res.*, *115*, A10225, doi:10.1029/2010JA015625.
- Li, S.-S., V. Angelopoulos, A. Runov, X.-Z. Zhou, J. McFadden, D. Larson, J. Bonnell, and U. Auster (2011), On the force balance around dipolarization fronts within bursty bulk flows, *J. Geophys. Res.*, doi:10.1029/2010JA015884, in press.
- Nakamura, R., et al. (2004), Spatial scale of high-speed flows in the plasma sheet observed by Cluster, *Geophys. Res. Lett.*, *31*, L09804, doi:10.1029/2004GL019558.
- Ohtani, S., M. A. Shay, and T. Mukai (2004), Temporal structure of the fast convective flow in the plasma sheet: Comparison between observations and two-fluid simulations, *J. Geophys. Res.*, *109*, A03210, doi:10.1029/2003JA010002.
- Ohtani, S., H. J. Singer, and T. Mukai (2006), Effects of the fast plasma sheet flow on the geosynchronous magnetic configuration: Geotail and GOES coordinated study, *J. Geophys. Res.*, *111*, A01204, doi:10.1029/2005JA011383.
- Panov, E. V., et al. (2010), Multiple overshoot and rebound of a bursty bulk flow, *Geophys. Res. Lett.*, *37*, L08103, doi:10.1029/2009GL041971.
- Pontius, D. H., Jr., and R. A. Wolf (1990), Transient flux tubes in the terrestrial magnetosphere, *Geophys. Res. Lett.*, *17*(1), 49–52.
- Schödel, R., W. Baumjohann, R. Nakamura, V. A. Sergeev, and T. Mukai (2001), Rapid flux transport in the central plasma sheet, *J. Geophys. Res.*, *106*, 301–313.
- Shiokawa, K., W. Baumjohann, and G. Haerendel (1997), Braking of high-speed flows in the near-Earth tail, *Geophys. Res. Lett.*, *24*(10), 1179–1182.
- Sibeck, D. G., and V. Angelopoulos (2008), THEMIS science objectives and mission phases, *Space Sci. Rev.*, *141*, 35–59, doi:10.1007/s11214-008-9393-5.
- Takada, T., R. Nakamura, W. Baumjohann, Y. Asano, M. Volwerk, T. L. Zhang, B. Klecker, H. Rème, E. A. Lucack, and C. Carr (2006), Do BBFs contribute to inner magnetosphere dipolarizations: Concurrent Cluster

- and Double Star observations, *Geophys. Res. Lett.*, *33*, L21109, doi:10.1029/2006GL027440.
- TanDokoro, R., and M. Fujimoto (2005), Three-dimensional MHD simulation study of the structure at the leading part of a reconnection jet, *Geophys. Res. Lett.*, *32*, L23102, doi:10.1029/2005GL024467.
- Tsyganenko, N. A., and D. H. Fairfield (2004), Global shape of the magnetotail current sheet as derived from Geotail and Polar data, *J. Geophys. Res.*, *109*, A03218, doi:10.1029/2003JA010062.
- Wolf, R. A., V. Kumar, F. R. Toffoletto, G. M. Erickson, A. M. Savoie, C. X. Chen, and C. L. Lemon (2006), Estimating local plasma sheet  $PV^{5/3}$  from single-spacecraft measurements, *J. Geophys. Res.*, *111*, A12218, doi:10.1029/2006JA012010.
- Wolf, R. A., Y. Wan, X. Xing, J.-C. Zhang, and S. Sazykin (2009), Entropy and plasma sheet transport, *J. Geophys. Res.*, *114*, A00D05, doi:10.1029/2009JA014044.
- Yang, J., F. R. Toffoletto, G. M. Erickson, and R. A. Wolf (2010), Superposed epoch study of  $PV^{5/3}$  during substorms, pseudobreakups and convection bays, *Geophys. Res. Lett.*, *37*, L07102, doi:10.1029/2010GL042811.
- 
- V. Angelopoulos and A. Runov, Institute of Geophysics and Planetary Physics, University of California, 3845 Slichter Hall, Los Angeles, CA 90095-1567, USA.
- S. Apatenkov, S. Dubyagin, and V. Sergeev, Earth Physics Department, St. Petersburg State University, Ulyanovskaya 1, Petrodvoretz, St. Petersburg 198504, Russia. (stepan@geo.phys.spbu.ru)
- W. Baumjohann and R. Nakamura, Space Research Institute, Austrian Academy of Sciences, Schmiedlstraße 6, A-8042 Graz, Austria.
- D. Larson and J. McFadden, Space Sciences Laboratory, University of California, 7 Gauss Way, Berkeley, CA 94720-7450, USA.